

Hydrodynamic Characteristics of Inverse T-Type Floating Breakwaters

Esmaeel Masoudi*

* M.Sc., Amirkabir University of Technology; Department of Maritime Engineering
Esmaeelmasoodi@aut.ac.ir

ARTICLE INFO

Article History:

Received: 6 Feb. 2019

Accepted: 16 Mar. 2019

Keywords:

Floating breakwater

Rectangular cross section

Transmission coefficient

Reflection coefficient

Inverse T-type

ABSTRACT

Various types of floating breakwaters in different configuration and shapes are used to reduce wave height in coastal areas. The most important parameter in designing breakwaters are their shapes which determines hydrodynamic reaction to incident waves. Some cross sections are more effective and more efficient than others. In framework of numerical methods, finite element and boundary element methods are two popular and effective approaches which have been widely applied to floating body problems. In this study by using boundary element method, diffraction problem is solved for a new type of breakwater, which is called inverse T-type floating breakwater. To have a validated results, a rectangular cross section floating breakwater is analyzed and results are compared to previous researches. The final goal of this study is obtaining hydrodynamic characteristics of this new type of breakwater and comparing its response to sinusoidal waves with other conventional floating breakwaters. It is shown that in same weight, this new type of breakwater has better transmission coefficient among other conventional breakwaters and might be used as an efficient alternative.

1. Introduction

The development of coastal or inland waters may often depend on sea behavior at a specific site and breakwaters of various dimensions and configurations have been widely employed to increase the use of locations exposed to wave attack. The purpose of installing a breakwater is to reduce the height of the incident waves to an acceptable level in respect to the intended use of the site on their leeward side. The increase in the number of private pleasure crafts as well as diving safe zones has generated an increasing demand for more protected sites. Fixed breakwaters has been widely used to attenuate surface water waves. Total costs and transmitted wave's height are often dictate possible breakwater alternatives. Because of environmental and economic concerns, floating breakwaters, FBs, are developed recently as a substitution to fixed breakwaters. The FB usually consists of a floating pontoon with finite draft which exposed to water waves. The movement of the FB can be limited to three degrees of freedom e.g., sway, heave and roll.

There are three methods which have been applied to study floating structures in different conditions: numerical methods, experimental methods and analytical methods. Analytical methods in studying floating structures firstly developed by Garrett [1], in

which wave forces and moments on a floating dock was calculated. Other researchers such as Black et.al [2], Hulme [3], Wu and Taylor [4], Bergren and Johnson [5], Lee [6], Hsu and Wu [7], Zheng et al [8, 9], Masoudi & Zeraatgar [10] and Deng et.al [11] also used analytical methods to investigate floating structures problem. Analytic solution consists of separating the domain to sub-domains, then obtaining velocity potentials in each sub-domain approximated with orthogonal functions. After satisfying the boundary conditions and the common boundaries between sub-domains, the unknown coefficients in orthogonal functions are obtained and the velocity potentials become implicit in each sub-domain. Having determined the velocity potentials, wave characteristics in both sides of the structure and therefore, the transmission and reflection coefficients will be obtained.

A well-known example of experimental method is Sannasiraj et al. [12] in which mooring forces and motions have been considered for a pontoon type breakwater. Examples of recent experimental methods are Christensen et al. [13] in which FBs with effect of wing plates are studied and C. Ji et al. [14] that discussed hydrodynamic behavior of double row FBs in a wave flume under regular wave action.

In framework of numerical methods, finite element and boundary element methods are two popular and

effective approaches which have been widely applied to floating body problems. Examples of numerical methods are using finite - infinite element method by Li et al [15], using boundary element method for studying floating structures by Yamamoto et al [16] and using boundary element method for solving potential equation by Masoudi and Zeraatgar [17] and Masoudi [18] in which various kinds of floating breakwaters are studied and best cross section among them were determined. Zhan et al. [19] are also investigate fluid structure interaction between an inverse T-type FB and regular/irregular waves and Zhang et.al [20] use viscous flow simulation of wave-body interactions for rectangular and inverse π type floating breakwaters.

In this study, a new type of FB say inverse T-type FB in water of finite depth and extent will be analyzed using boundary element software ANSYS AQWA in regular sinusoidal waves. In order to validate the results, other researcher results such as Masoudi & Zeraatgar [10], Zheng et al [8] and Black et al [2] are used. Then hydrodynamic characteristics of the introduced breakwater will be analyzed. Exiting forces as well as transmission and reflection coefficient will be determined in inverse T-type FB and will be compared to conventional rectangular breakwater. Final goal of this study is determining whether this new type of floating breakwater is better than other conventional floating breakwaters or not.

Afterward, a parametric study will be done to extract comprehensive view of hydrodynamic behavior of this type of breakwater. Comprehensive understanding of most important parameters on the efficiency of the breakwater will be investigated.

2. Method and Material

For large ratio of length of the breakwater to the wavelength, the fluid is assumed incompressible and irrotational. There will be a scalar function which known as velocity potential, ϕ , that satisfies the Laplace equation as shown in equation (1). Also the velocity components and pressure can be obtained using equations (2) and (3).

$$\nabla^2 \phi = 0 \quad (1)$$

$$\frac{\partial \phi}{\partial x} = u \quad \frac{\partial \phi}{\partial y} = v \quad \frac{\partial \phi}{\partial z} = w \quad (2)$$

$$P = -\rho \left(\frac{\partial \phi}{\partial t} + \frac{1}{2} \nabla \phi^2 + gz \right) + c(t) \quad (3)$$

In which u, v, w are velocities in x, y, z directions respectively. Also P is pressure and $c(t)$ is a constant. Basic configuration of the breakwater and the arrangement of coordinate system are shown in Figure 1. It is assumed that a linear wave with height of H and circular frequency of $\omega = \frac{2\pi}{T}$ propagates to the positive x direction with θ angle. The total potential of the problem can be separated in three parts. First one is

the incident wave potential of linear waves which considered independently from existence of the breakwater given by:

$$\phi_I = -\frac{igA \cosh[k(z+h)]}{\omega \cosh(kh_1)} \exp(ikx \cos \theta) \quad (4)$$

In which:

$$\omega^2 = gk \tanh kh \quad (5)$$

Second one is the diffraction potential (ϕ_d), which induced by interaction of incident wave and the breakwater, and the third is the induced potential from motions of the structure in three degrees of freedom which known as radiation potentials (ϕ_r).

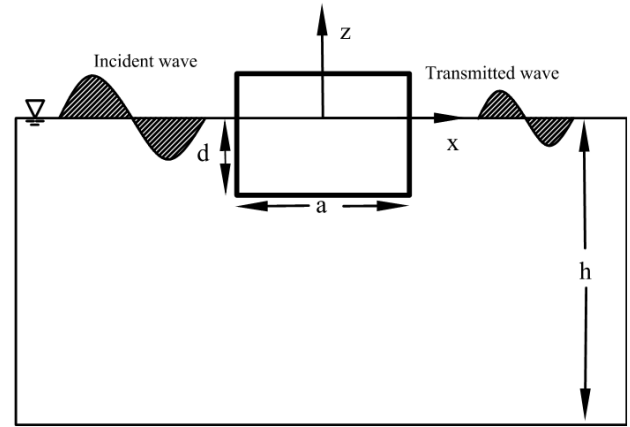


Figure 1. Basic configuraion, coordinate system of a typical floating breakwater problem

Referring to Figure 1, the problem is considered as a 2D case, motions are restricted in three degrees of freedom which are sway, heave and roll as specified with indices 1, 2 and 3, respectively. The total potential, ϕ_t , expressed as follows:

$$\phi_t = \phi_i + \phi_d + \sum_{l=1}^3 \phi_r^l \quad (6)$$

By dividing the total problem in two parts, boundary conditions and formulation for each part can be clarified as follows:

2.1. Diffraction problem

The linear diffraction problem and its boundary conditions can be expressed by oscillatory function, ϕ_d , given by:

$$\phi_d(x, z, y) = \phi_d(x, z) \exp(iky \sin \theta) \quad (7)$$

$$\frac{\partial \phi_d}{\partial z} - \frac{\omega^2}{g} \phi_d = 0 \quad (z = 0) \quad (8)$$

$$\frac{\partial \phi_d}{\partial z} = 0 \quad (z = -h) \quad (9)$$

$$\frac{\partial \phi_d}{\partial n} = -\frac{\partial \phi_i}{\partial n} \quad (\text{on } S_0) \quad (10)$$

$$\lim_{x \rightarrow \infty} \left[\frac{\partial \phi_d}{\partial x} \pm ik \cos \theta \phi_d \right] = 0 \quad (11)$$

The boundary value problem for the diffraction potential is defined by governing Laplace equation and the boundary conditions are defined in equations (8) to (12). Where n is the unit normal vector outward the body, S_0 is the wetted surface and h is the water depth as shown in Figure 1.

2.2. Radiation problem

In the framework of the linear theory, the radiation problem and its boundary conditions can also be described by the following oscillatory radiation potential:

$$\phi_R^l(x, z, y) = -i\omega A_R^l \phi_R^l(x, z) \exp(iky \sin \theta) \quad (12)$$

$$\frac{\partial \phi_R^l}{\partial z} - \frac{\omega^2}{g} \phi_R^l = 0 \quad (z = 0) \quad (13)$$

$$\frac{\partial \phi_R^l}{\partial z} = 0 \quad (z = -h) \quad (14)$$

$$\frac{\partial \phi_R^l}{\partial z} = \delta_{1,L} - (x - x_0) \delta_{3,L} \quad (z = -d \quad |x| \leq a/2) \quad (15)$$

$$\frac{\partial \phi_R^l}{\partial x} = \delta_{2,L} + (z - z_0) \delta_{3,L} \quad (-d \leq z \leq 0 \quad |x| = a/2) \quad (16)$$

$$\lim_{x \rightarrow \infty} \left[\frac{\partial \phi_R^l}{\partial x} \pm ik \cos \theta \phi_R^l \right] = 0 \quad (17)$$

$$\delta_{i,j} = \begin{cases} 1 & i = j \\ 0 & i \neq j \end{cases} \quad (18)$$

The amplitude of motion mode, L , of the structure is denoted by A_R^l and (x_0, z_0) is the center of rotation, which can be either center of coordinate system or the center of gravity. The boundary value problem for the linear radiation potential, can be defined by governing Laplace equation and the boundary condition as defined in equations (13) to (18).

3. Results

3.1. Verification of results

ANSYS Software Pack provides complete simulation of offshore structures in regular and irregular waves. In order to assess the simulation, a rectangular cross section breakwater floating in sinusoidal waves of finite depth is considered. Figure 2 shows the results for wave induced forces on the breakwater for a domain of $(\frac{a}{d} = \frac{h}{d} = 2)$. The results are compared with studies of Masoudi and Zeraatgar [10], Zheng et al. [8] and Black et al. [2].

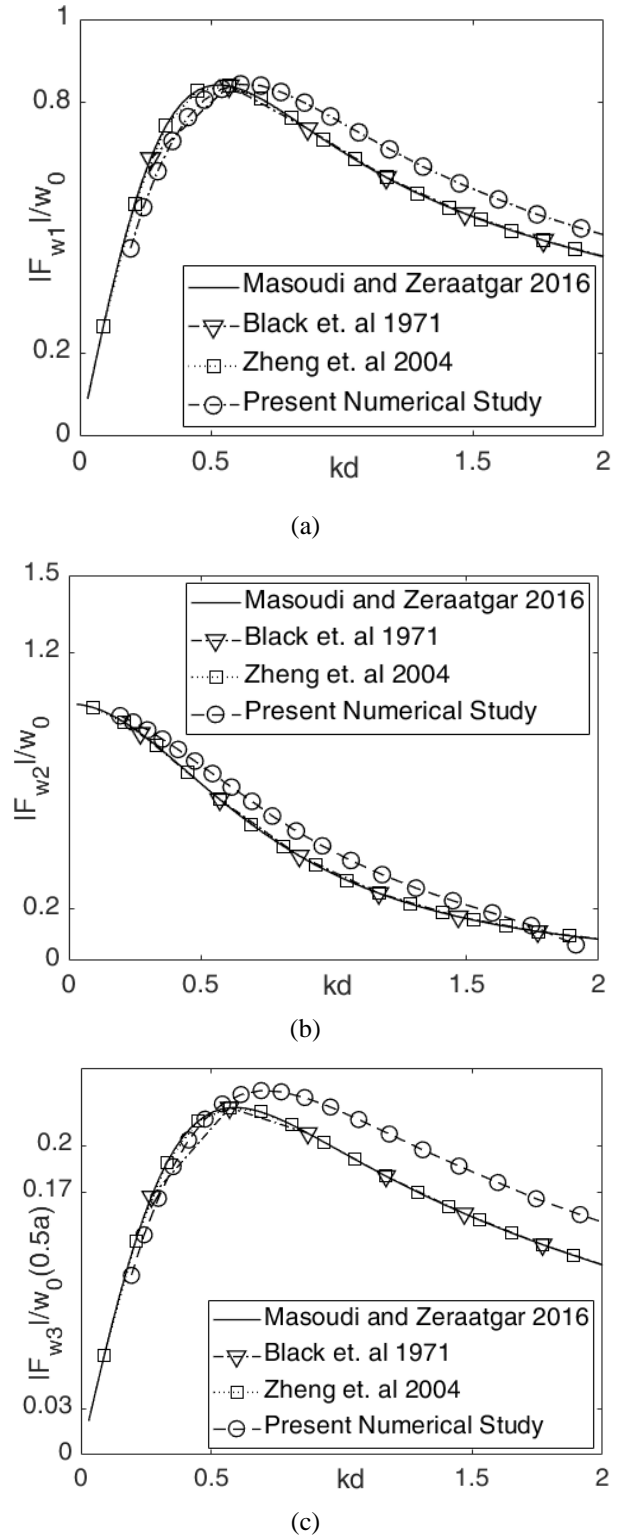


Figure 2. A comparison between present numerical study to other researches for a rectangular FB in a domain of $(\frac{a}{d} = \frac{h}{d} = 2)$ - (a) Horizontal force, (b) vertical force, (c) moment

In Figure 2, forces induced to the breakwater say F_{w1}, F_{w2}, F_{w3} are non – dimensioned with $w_0 = \rho g A a$, in which ρ, g and A are water density, gravity acceleration and incident wave amplitude respectively. It could be concluded that the wave forces in three directions imposed on breakwater of the present study are quite comparable with other studies.

3. 2. Inverse T-type FB

Figure. 3 shows general configuration of an inverse T-type FB. Parameters e and f are defined symmetrically in the breakwater. In order to make a good comparison parameters are defined similar to Figure 1. Equation (6) still valid and basic formulation are defined according to equations (19) to (24) for diffraction problem and equations (25) to (31) for radiation problem.

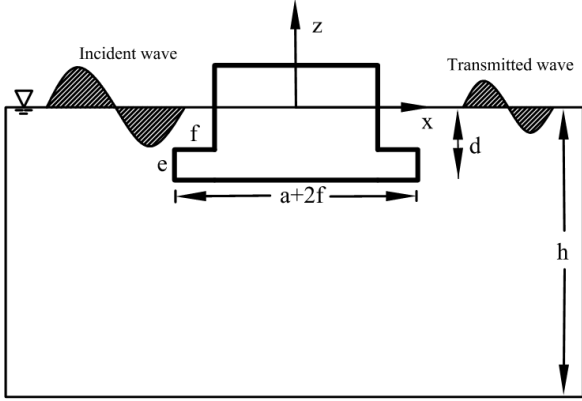


Figure 3. Basic configuraion of an inverse T-type FB

$$\phi_D(x, z, y) = \phi_D(x, z) \exp(iky \sin \theta) \quad (19)$$

$$\frac{\partial \phi_D}{\partial z} - \frac{\omega^2}{g} \phi_D = 0 \quad (z = 0) \quad (20)$$

$$\frac{\partial \phi_D}{\partial z} = 0 \quad (z = -h) \quad (21)$$

$$\frac{\partial \phi_D}{\partial n} = -\frac{\partial \phi_I}{\partial z} \quad \left(z = -d, |x| \leq \frac{a}{2} + f \right) \quad (22)$$

$$(z = -d + e, -\frac{a}{2} - f \leq x \leq -\frac{a}{2}) \quad (22)$$

$$(z = -d + e, \frac{a}{2} \leq x \leq \frac{a}{2} + f) \quad (22)$$

$$\frac{\partial \phi_D}{\partial x} = -\frac{\partial \phi_I}{\partial n} \quad (\text{on } S_0) \quad (23)$$

$$\lim_{x \rightarrow \infty} \left[\frac{\partial \phi_D}{\partial x} \pm ik \cos \theta \phi_D \right] = 0 \quad (24)$$

$$\phi_R^L(x, z, y) = -i\omega A_R^L \phi_R^L(x, z) \exp(iky \sin \theta) \quad (25)$$

$$\frac{\partial \phi_R^L}{\partial z} - \frac{\omega^2}{g} \phi_R^L = 0 \quad (z = 0) \quad (26)$$

$$\frac{\partial \phi_R^L}{\partial z} = 0 \quad (z = -h) \quad (27)$$

$$\frac{\partial \phi_R^L}{\partial z} = \delta_{1,L} - (x - x_0) \delta_{3,L} \quad (28)$$

$$(z = -d, |x| \leq \frac{a}{2}) \quad (28)$$

$$(z = -d + e, -\frac{a}{2} - f \leq x \leq -\frac{a}{2}) \quad (28)$$

$$(z = -d + e, \frac{a}{2} \leq x \leq \frac{a}{2} + f) \quad (28)$$

$$\frac{\partial \phi_R^L}{\partial x} = \delta_{2,L} + (z - z_0) \delta_{3,L} \quad (29)$$

$$(-d + e \leq z \leq 0, |x| = \frac{a}{2}) \quad (29)$$

$$\lim_{x \rightarrow \infty} \left[\frac{\partial \phi_R^L}{\partial x} \pm ik \cos \theta \phi_R^L \right] = 0 \quad (30)$$

$$\delta_{i,j} = \begin{cases} 1 & i = j \\ 0 & i \neq j \end{cases} \quad (31)$$

To make a comparison between hydrodynamic behavior of an inverse T-type FB and the conventional FB, Figure 4 is shown considering $\frac{a}{d} = \frac{h}{d} = 2$ and $\frac{f}{a} = \frac{e}{d} = 0.5$. Figure 4 (a), (b) and (c) are exiting forces in sway, heave and roll direction respectively.

Transmission coefficient (T_w) is defined as the amplitude of transmitted wave to the amplitude of the incident wave. Also, reflection coefficient (R_w) is defined as the amplitude of reflected wave to the amplitude of the incident wave. Longuet-Higgins [21] proposed the horizontal drift force (F_d) directly in terms of the reflection coefficient as follows:

$$F_d = \frac{Ec_g}{c} (1 + R_w^2 - T_w^2) = \frac{2Ec_g}{c} R_w^2 \quad (32)$$

According to equation (32), it is possible to calculate mean drift force on the body and then derive transmission and reflection coefficients. In this way, transmission and reflection coefficients of rectangular and inverse T-type FBs are shown in Figure 5 considering $\frac{a}{d} = \frac{h}{d} = 2$ and $\frac{f}{a} = \frac{e}{d} = 0.5$. It should be noted that, for making a logical comparison, in cases displayed in Figure 4 and Figure 5, breakwaters share same weight.

3. 3. Parametric study on the inverse T-type FB

According to Figure 3, main parameters to be considered in the effectiveness of this type of breakwater are e and f . Considering their definition, when these parameters converges to zero, FB's hydrodynamic behavior must converge to the rectangular type. However, the trend of fundamental hydrodynamic performances with respect to the change of these parameters should be determined. For better display, parameters are non-dimensioned as $\frac{e}{d}$ and $\frac{f}{a}$. Figure 6 shows exiting force changes with respect to the change of $\frac{e}{d}$ and $\frac{f}{a}$. Figure 6 (a, c, e) displays $\frac{e}{d}$ effect, while Figure 6 (b, d, f) depicts $\frac{f}{a}$ effects. For all cases in Figure 6 it is assumed that $(\frac{a}{d} = \frac{h}{d} = 2)$. Furthermore for (a), (c) and (e) it is considered that $(\frac{f}{a} = 0.5)$ and for (b), (d) and (f) it is assumed that $\frac{e}{d} = 0.5$. For having more comprehensive view of hydrodynamic characteristic of the inverse T-type FB, Figure 7 is shown. Transmission coefficient and reflection coefficient are depicted for different values of $\frac{e}{d}$ and $\frac{f}{a}$. The method for extracting these coefficients are same as section 3.2. It should be noted that for all case studies in Figure 6 and Figure 7 it is assumed that breakwater's weight remains constant.

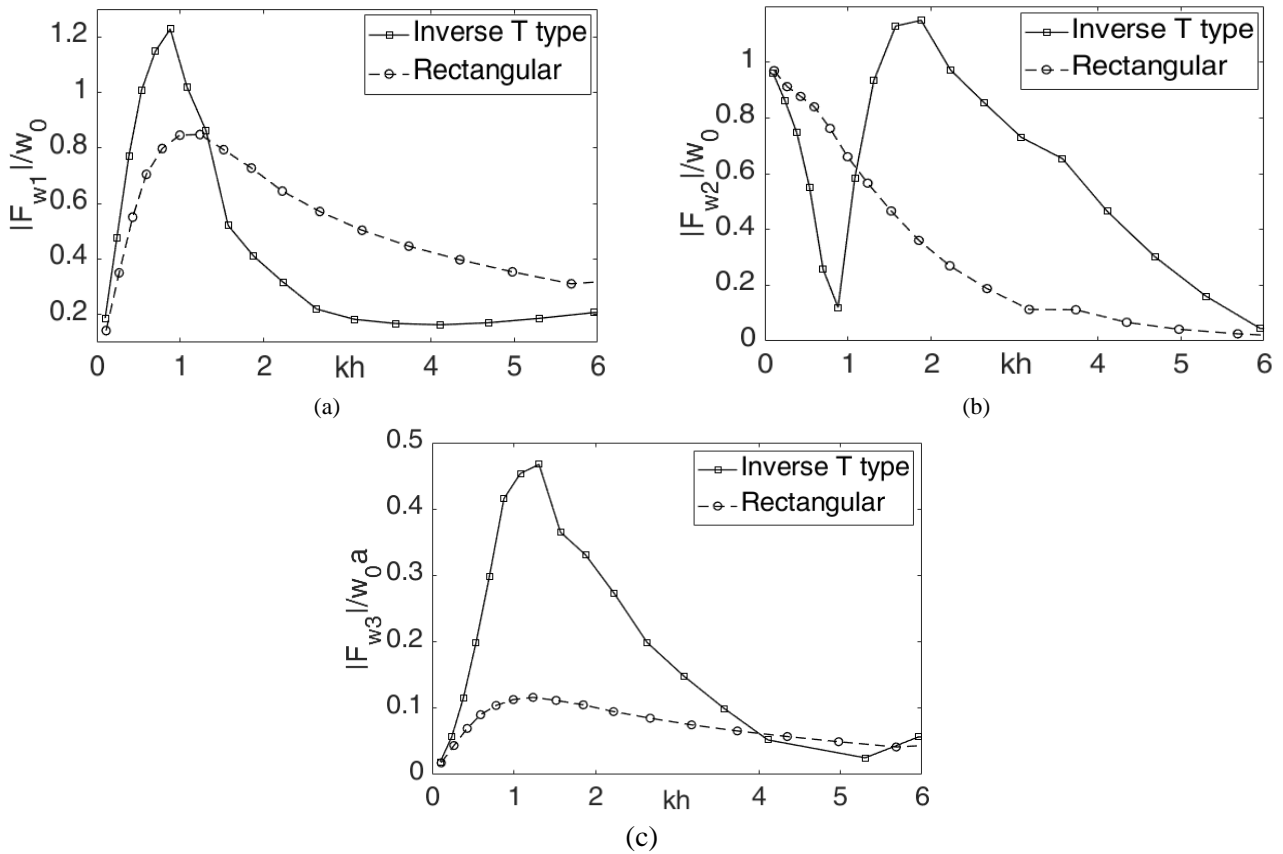


Figure 4. Exiting forces in sway (a), heave (b) and roll (c) directions for rectangular and inverse T-type FB ($\frac{a}{d} = \frac{h}{d} = 2$) and ($\frac{f}{a} = \frac{e}{d} = 0.5$)

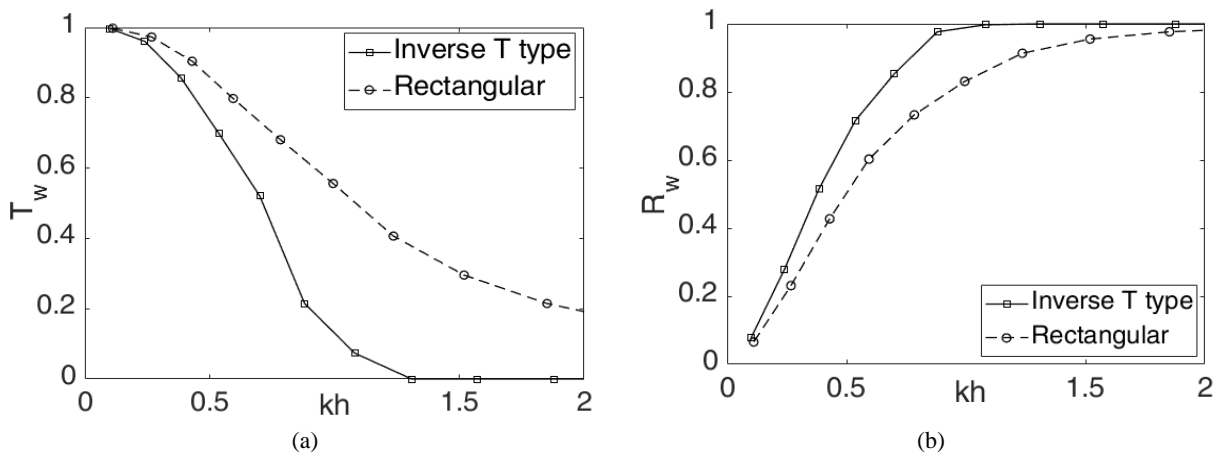
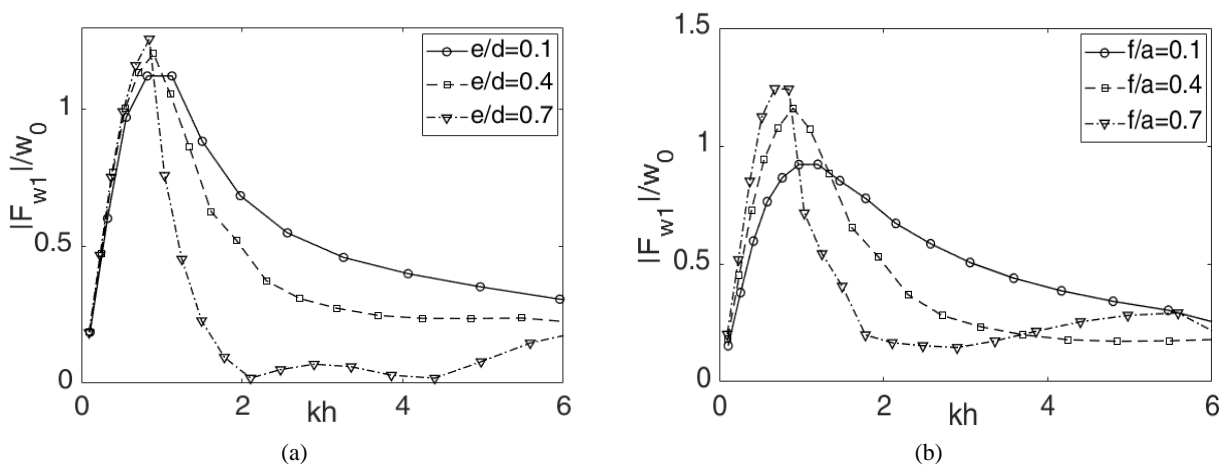


Figure 5. Transmission (a), and reflection (b) coefficients for rectangular and inverse T-type FB ($\frac{a}{d} = \frac{h}{d} = 2$) and ($\frac{f}{a} = \frac{e}{d} = 0.5$)



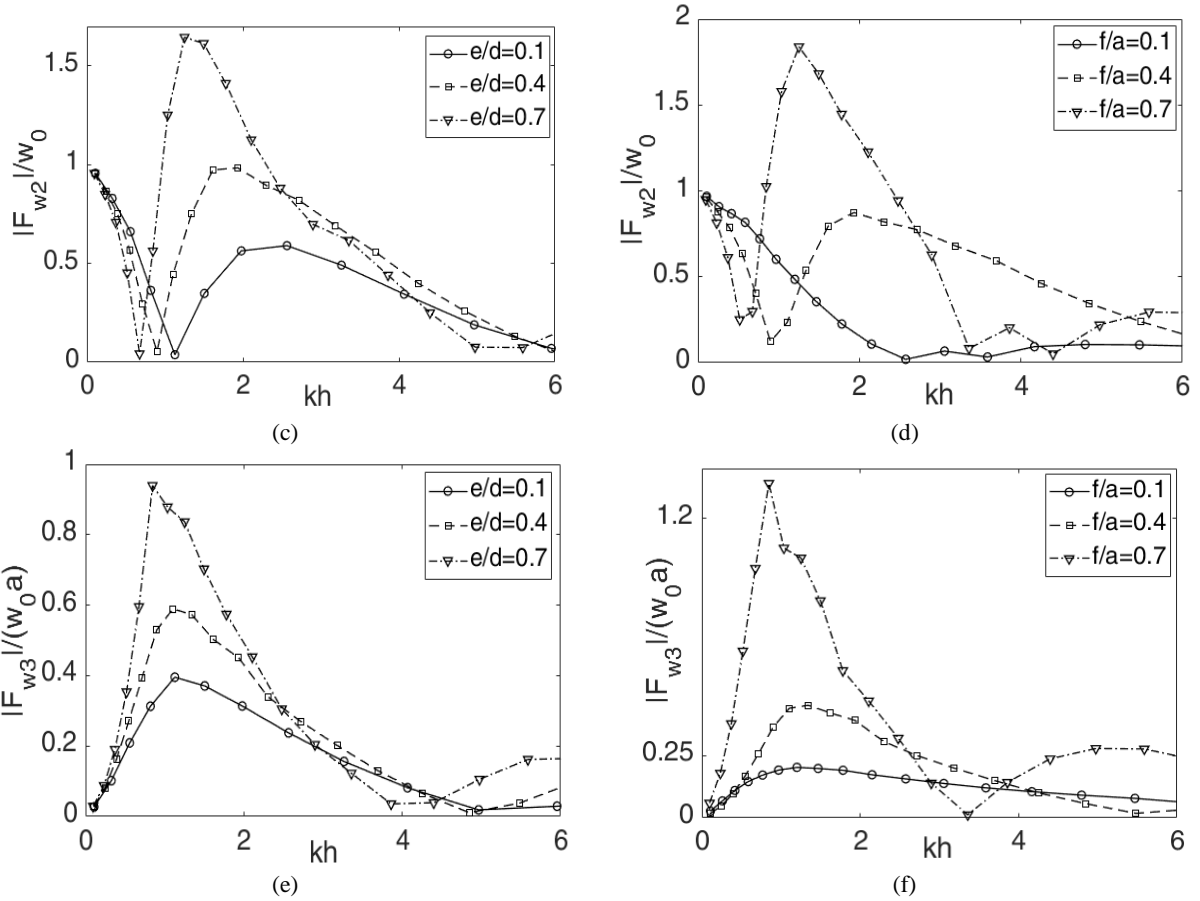


Figure 6. Exiting forces parametric study for e/d (a, c, e) and f/a (b, d, f)

$$\left(\frac{a}{d} = \frac{h}{d} = 2\right) \& \left(\frac{f}{a} = 0.5 \text{ for } (a, c, e), \frac{e}{d} = 0.5 \text{ for } (b, d, f)\right)$$

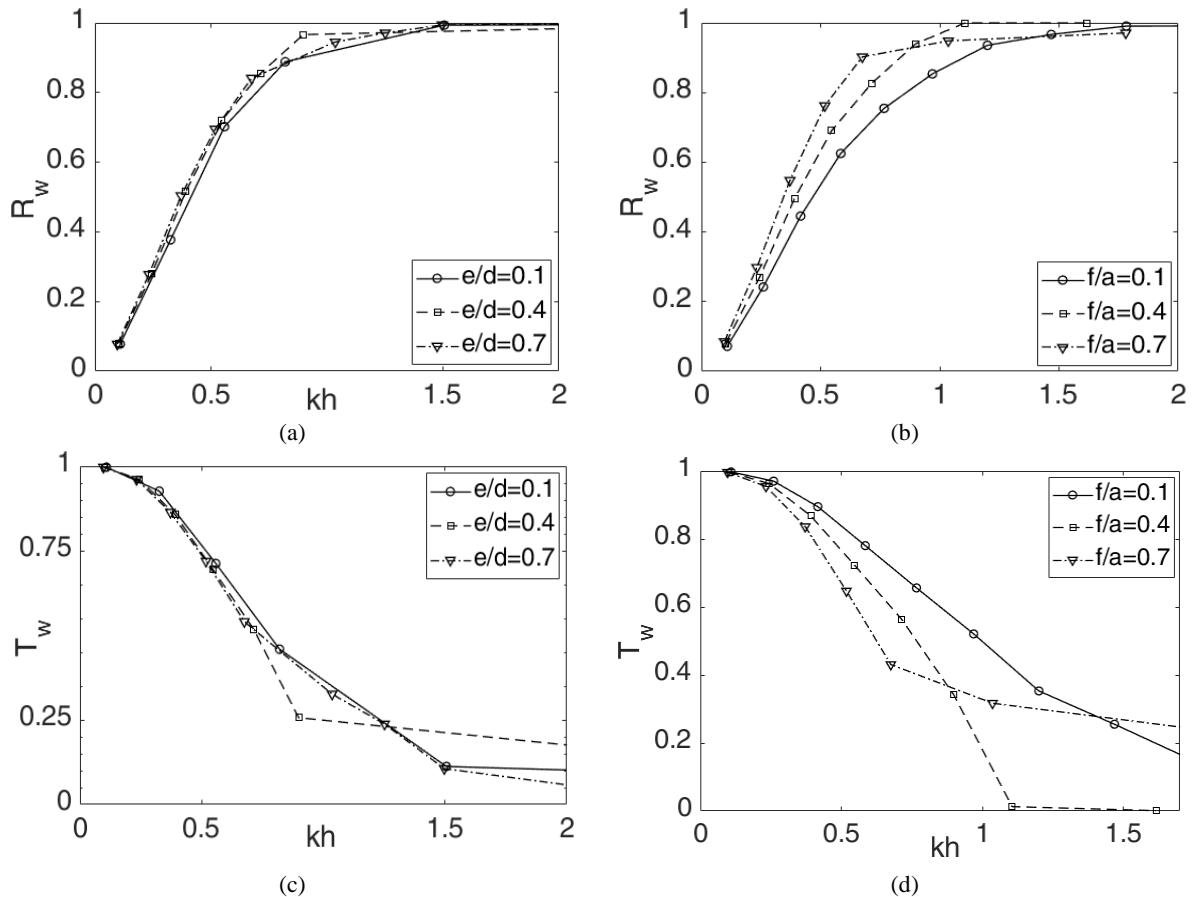


Figure 7. Reflection (a, b) and Transmission (c, d) coefficients parametric study

$$\left(\frac{a}{d} = \frac{h}{d} = 2\right) \& \left(\frac{f}{a} = 0.5 \text{ for } (a, c), \frac{e}{d} = 0.5 \text{ for } (b, d)\right)$$

4- Discussion

Considering Figure 4, it can be concluded that inverse T-type FB's exiting forces in roll direction is much higher than rectangular FB. For industrial purposes, considering mooring designs it would be a negative impact. On the other hand, exiting forces in sway direction for inverse T-type FB is larger than rectangular FB for $kh < 1.2$. For other ranges of kh exiting forces in sway direction for rectangular FB is larger than inverse T-type FB. This trend for exiting forces in heave direction is completely vice versa. The author believe that $kh \sim 1.2$ is a critical number for this problem since maximum exiting moment also occur at this point.

Considering Figure 5, it can be concluded that inverse T-type FB absolutely display better hydrodynamic behavior encountering regular waves. Having known the fact that both breakwaters share same weight, large difference between transmission coefficients for rectangular FB and inverse T-type FB purely is a result of their shape. Another fact that can be obtained from this Figure is that in $kh \sim 1.2$ the transmission coefficient for inverse T-type FB reaches zero which is compatible with definition of critical point in above paragraph.

Figure 6 demonstrate parametric study considering $\frac{e}{a}$ and $\frac{f}{a}$ as main parameters for inverse T-type FB. First, it is obvious that for every breakwater, there is a critical point which happen in the range of $0 \leq kh \leq 2$. At this point, maximum exiting moment (in roll direction) happens. Also, it is patent that for $\frac{f}{a} = 0.1$ (where $\frac{e}{a} = 0.5$) the inverse T-type FB exiting forces are similar to rectangular FB, while for cases that $\frac{e}{a} = 0.1$ (where $\frac{f}{a} = 0.5$) it is not. So it can be concluded that the $\frac{f}{a}$ parameter is much more important than $\frac{e}{a}$ parameter in hydrodynamic behavior of the inverse T-type FB.

Finally, Figure 7 that demonstrate effectiveness of parameters $\frac{e}{a}$ and $\frac{f}{a}$ confirms the fact that at same weight, $\frac{f}{a}$ is a more important factor in hydrodynamic efficiency of the inverse T-type FB. It is obvious that increasing the value of $\frac{f}{a}$ results in decreasing transmission coefficient which results in better efficiency.

5- Conclusion

In this study, hydrodynamic characteristics of the inverse T-type floating breakwater is analyzed using boundary element method software. As far as validation of results were concerned, outputs were compared to previous prominent researches and good agreement were achieved. Then exiting forces as well as transmission and reflection coefficients of the inverse T-type FB and rectangular FB are compared. Results show that, at the same weight, the inverse T-type FB show lower transmission coefficient and so demonstrate higher efficiency. Finally a parametric

study is carried out in order to fully comprehend hydrodynamic behavior of the inverse T-type FB. It is shown that parameter $\frac{f}{a}$ play an essential role in the efficiency of the inverse T-type FB and should be critically considered in design stage.

6- References

- 1- C. Garrett, 1971. *Wave forces on a circular dock*, Journal of Fluid Mechanics, 46, 129-139
- 2- Black, J.L., Mei, C.C. and Bray, M.C.G., 1971. *Radiation and scattering of water waves by rigid bodies*. Journal of Fluid Mechanics, 46(1), 151-164
- 3- A. Hulme, 1982. *The wave forces acting on a floating hemisphere undergoing forced periodic oscillations*, Journal of Fluid Mechanics, 121, 443-463
- 4- G. Wu and R. E. Taylor, 1990. *The second order diffraction force on a horizontal cylinder in finite water depth*, Applied Ocean Research, 12, 106-111
- 5- L. Berggren and M. Johansson, 1992. *Hydrodynamic coefficients of a wave energy device consisting of a buoy and a submerged plate*, Applied Ocean Research, 14, 51-58
- 6- J.-F. Lee, 1995. *On the heave radiation of a rectangular structure*, Ocean Engineering, 22, 19-34
- 7- H. Hsu and Y.-C. Wu, 1997. *The hydrodynamic coefficients for an oscillating rectangular structure on a free surface with sidewall*, Ocean Engineering, 24, 177-199
- 8- Zheng, Y.H., You, Y.G. and Shen, Y.M., 2004. *On the radiation and diffraction of water waves by a rectangular buoy*. Ocean engineering, 31(8-9), 1063-1082
- 9- Zheng, Y.H., Shen, Y.M., You, Y.G., Wu, B.J. and Jie, D.S., 2004. *On the radiation and diffraction of water waves by a rectangular structure with a sidewall*. Ocean Engineering, 31(17-18), 2087-2104
- 10- Masoudi, E, Zeraatgar, H., (2015), *Application of method of separation of variables for analyzing floating breakwater*, IJMT, Vol (11) / No.22
- 11- Deng, Z., Wang, L., Zhao, X., & Huang, Z., (2019), *Hydrodynamic performance of a T-shaped floating breakwater*. Applied Ocean Research, 82, 325-336.
- 12- Sannasiraj, S.A., Sundar, V. and Sundaravadivelu, R., 1995. *The hydrodynamic behaviour of long floating structures in directional seas*. Applied Ocean Research, 17(4), 233-243
- 13- Christensen, E.D., Bingham, H.B., Friis, A.P.S., Larsen, A.K. and Jensen, K.L., 2018. *An experimental and numerical study of floating breakwaters*. Coastal Engineering, 137, 43-58
- 14- Ji, C., Deng, X. and Cheng, Y., 2018. *An experimental study of double-row floating breakwaters*. Journal of Marine Science and Technology, 1-13
- 15- B. Li, S. Lau, and C. Ng, (1991), *Second order wave diffraction forces and run up by finite-infinite*

element method, applied ocean research, vol. 13, 270-286

16- T. Yamamoto, A. Yoshida, and T. Ijima, (1980), *Dynamics of elastically moored floating objects*, applied ocean research, vol. 2, 85-92

17- E. Masoudi, H. Zeraatgar, 2017. *Hydrodynamic Analysis of Various Cross Sections of Floating Breakwaters*, Proceedings of 7th international offshore industries conference (Sharif University of technology, Tehran, Iran), pp. 82

18- E. Masoudi, 2016. *Hydrodynamic study of Various Cross Sections of Floating Breakwaters*, Proceedings of 18th marine industries conference (Iranian Association of Naval architecture and Marine engineering, Kish, Iran), pp. 26

19- Zhan, J.M., Chen, X.B., Gong, Y.J. and Hu, W.Q., 2017. *Numerical investigation of the interaction between an inverse T-type fixed/floating breakwater and regular/irregular waves*. Ocean engineering, 137, 110-119

20- Zhang, X. S., Ma, S., & Duan, W. Y., (2018). *A new L type floating breakwater derived from vortex dissipation simulation*. Ocean Engineering, 164, 455-464.

21- Longuet-Higgins, M.S., 1977. *The mean forces exerted by waves on floating or submerged bodies with applications to sand bars and wave power machines*. Proceedings of the Royal Society of London. A. Mathematical and Physical Sciences, 352(1671), 463-480.